J. Eukaryot. Microbiol., 53(1), 2006 pp. 26–35

DOI: 10.1111/j.1550-7408.2005.00066.x

Transfer of the Members of the Genus *Brachiola* (Microsporidia) to the Genus *Anncaliia* Based on Ultrastructural and Molecular Data

CASPAR FRANZEN,[a] ELENA S. NASSONOVA,[b] JÜRGEN SCHÖLMERICH[a] and IRMA V. ISSI[c]

[a]*Department of Internal Medicine I, University of Regensburg, Regensburg, Germany, and*
[b]*Laboratory of Cytology of Unicellular Organisms, Institute of Cytology, Russian Academy of Sciences, and*
[c]*Laboratory of Microbiological Control, All-Russian Institute for Plant Protection, Russian Academy of Agricultural Sciences, St. Petersburg, Russia*

ABSTRACT. Two microsporidian genera, *Anncaliia* Issi, Krylova, & Nicolaeva 1993 and *Brachiola* Cali et al. 1998, possess a *Nosema*-type life cycle and unique cell surface ornamentations, which include precocious electron-dense coating of the plasmalemma and a variety of secretory structures deposited on the parasite surface and scattered in the host cell cytoplasm. Comparative analysis of ultrastructure of *Anncaliia meligethi* (the type species of the genus *Anncaliia*) and of *B. vesicularum* and *B. algerae* (the best-studied members of the genus *Brachiola*) clearly demonstrated that these microsporidia share many distinctive morphological features. The comparison of small subunit ribosomal DNA sequences showed high sequence identity of *A. meligethi* and *B. algerae*. Phylogenetic analyses indicated that the rDNA sequences of *A. meligethi* clustered with those of *B. algerae* suggesting a close relatedness of these microsporidia. The combination of molecular and morphological data provided clear evidence that these microsporidia belong to the same genus and therefore, warranted emendation of the genus *Anncaliia* and establishments of the following new combinations: *Anncaliia vesicularum* nov. comb., *Anncaliia algerae* nov. comb., *Anncaliia connori* nov. comb., and *Anncaliia gambiae* nov. comb.. The generic name *Brachiola* is submerged according to the rule of priority.

Key Words. *Anncaliia*, *Brachiola*, microsporidia, rDNA, taxonomy.

THE genus *Anncaliia* Issi, Krylova, & Nicolaeva 1993 was established to accommodate two microsporidian species that were previously assigned to the genus *Nosema* (Issi, Krylova, and Nicolaeva 1993). The type species of the genus, *Anncaliia meligethi*, formerly *Nosema meligethi* Issi & Radishcheva 1979, was isolated from the pollen beetle *Meligethes aeneus* (Coleoptera: Nitidulidae). The second species, *Anncaliia varivestis*, previously *Nosema varivestis* Brooks, Hazard, & Becnel 1985, is a microsporidium from the Mexican bean beetle *Epilachna varivestis* (Coleoptera: Coccinellidae). These species shared the principal defining characters of the genus *Nosema*: development in direct contact with host cell cytoplasm, diplokaryotic nuclei, and disporoblastic sporogony. However, they displayed unique cell surface structures and a number of other distinctive morphological features allowing their differentiation from *Nosema* spp. In contrast to typical *Nosema* species, the developmental stages of *Anncaliia* spp., including the earliest proliferative ones, possessed a supplementary surface coat consisting of tubular structures and secretory granules. Derivatives of the structures appeared scattered in the cytoplasm of infected cells. Additionally, unlike *Nosema* spp., the polar tube in *Anncaliia* species was slightly anisofilar and the polaroplast was bipartite with an anterior lamellar part and a posterior tubular one (Issi et al. 1993).

Cali et al. (1998) isolated a microsporidium from a skeletal muscle biopsy specimen from an AIDS patient. This microsporidium was found to be a monomorphic, diplokaryotic species that developed in direct contact with the host cell cytoplasm. Sporogony was disporoblastic, producing spores with 7–10 coils of the polar filament arranged in one to three, usually two rows. The polar tube was anisofilar with the last two or three coils being thinner in diameter. All life-cycle stages were covered with a thick coat of electron-dense material deposited in vesiculotubular strands. Some proliferative cells elongated and produced protoplasmic extensions. Because this parasite was isolated from a patient with fever, it proliferated and produced spores at $\geq$37 °C. Although this microsporidium had many morphological and developmental features in common with the genus *Nosema*, its human body temperature tolerance together with such morphological characters as precocious thickening of the plasmalemma, the vesiculotubular appendages, and the presence of elongated protoplasmic extensions, led to the establishment of a new genus *Brachiola* with description of the type species *Brachiola vesicularum* Cali, Takvorian, Lewin, Rendel, Sian, Wittner, Tanowitz, Keohane, & Weiss 1998. The species *Nosema connori* Sprague 1974, a disseminated organism that caused malabsorption diarrhea in an athymic infant with a body temperature of 38.5 °C (Margileth et al. 1973; Strano, Cali, and Neafie 1976), was added as a second species to the genus *Brachiola*, and named *Brachiola connori* (Cali et al. 1998).

The appearance and progressive accumulation of electron-dense material on the surface of the plasmalemma indicate the beginning of sporogony in a vast majority of microsporidian species. Along with *Brachiola* spp., only a few microsporidia with a *Nosema*-like life cycle were known for the precocious occurrence of electron-dense material on the cell surface. These were the above-mentioned beetle-infecting *Anncaliia* spp. and *Nosema algerae* Vávra & Undeen 1970, a microsporidium originally described as a parasite of anopheline mosquitoes (Vávra and Undeen 1970) and other insect hosts (Undeen and Maddox 1973). Both *Anncaliia* spp. and *N. algerae* possessed external vesiculotubular structures, very similar to those of *B. vesicularum*. Nevertheless, Cali et al. (1998) dismissed consideration that *B. vesicularum* was a potential member of the genus *Anncaliia*, arguing that high-temperature tolerance is a distinguishing character (Cali et al. 1998). *Nosema algerae* was initially differentiated from *B. vesicularum* by three main criteria: (1) difference in thermotolerance (at that time *N. algerae* was thought to be intolerant of human body temperature), (2) wide tissue dissemination of *N. algerae* in mosquitoes vs. restriction of *B. vesicularum* to skeletal muscles in man, and (3) details of polar tube arrangement in spores. However, in the ensuing years these differences were shown to be not strictly tenable as in vitro cultures of *N. algerae* were shown to persist at 37 °C (Moura et al. 1999; Trammer et al. 1999) and its spores were found to have variable arrangements of the polar tube when grown at temperatures between 29 °C and 38 °C (Lowman, Takvorian, and Cali 2000; Trammer et al. 1999). Molecular phylogenetic analysis based on small subunit (SSU) and large subunit (LSU) ribosomal (r) RNA data demonstrated that sequences of *N. algerae* differ significantly from those of

Corresponding Author: C. Franzen, Department of Internal Medicine I, University of Regensburg, Regensburg, Germany—Telephone number: ++49-941-944-7169; FAX number: ++49-941-944-7123; e-mail: Caspar. Franzen@Klinik.Uni-Regensburg.de

the ''true'' *Nosema* species, including the type species *Nosema bombycis* (Baker et al. 1994; Müller et al. 2000). All these findings led to the taxonomic relocation of this microsporidium to the genus *Brachiola* (Lowman et al. 2000). Later, because of striking ultrastructural similarity, the microsporidium *Nosema* cf. *stegomyiae* sensu Fox and Weiser 1959, which infected natural and insectary colonies of the mosquitoes *Anopheles gambiae* and *Anopheles melas,* was transferred to the genus *Brachiola* and named *Brachiola gambiae* (Weiser and Žižka 2004).

Further studies indicated that *B. algerae* might cause infections of visceral tissues in humans (Cali, Weiss, and Takvorian 2004; Coyle et al. 2004; Visvesvara et al. 1999) and in immunodeficient mice (Koudela et al. 2001). It became evident that this microsporidium can grow at various temperatures and in various types of invertebrate and vertebrate hosts. This suggests the weakness of such physiological characters as thermotolerance for systematics of *Brachiola* spp. and of microsporidia in general. These considerations return us to the problem of the relationship between the genera *Anncaliia* and *Brachiola*. In this paper, we present ultrastructural and molecular data for *A. meligethi*, the type species of the genus *Anncaliia*, which clearly demonstrate that *Brachiola* spp. and *Anncaliia* spp. are congeneric.

MATERIALS AND METHODS

Parasite. Attempts to re-isolate *A. meligethi* from the beetle *M. aeneus* collected during spring and summer 2002 and 2003 in various locations in Russia and in Germany were not successful. Therefore, we used for DNA isolation archival air-dried specimens of *M. aeneus* stored at the State Collection of Entomopathogenic and Phytopathogenic Microorganisms and their Metabolites affiliated with the All-Russian Institute for Plant Protection RAAS (Podbelsky sh. 3, 189620 St. Petersburg, Pushkin, Russian Federation. Director: Prof. V. A. Pavljushin; curator: Dr. I. V. Boikova). Deposition number of the specimens is ST-GT-AM-R-1990. These beetles, collected in Kiev environs, Ukraine in May 1990, were heavily infected with *A. meligethi*. Specimens from the same population were used to study the ultrastructure of *A. meligethi* (Issi et al. 1993). The original electron micrographs were re-examined for the present study, and included electron micrographs of infected tissues of the caterpillar *Pieris brassicae* (Lepidoptera: Pieridae), experimentally infected with *A. meligethi* (Issi et al. 1993).

Transmission electron microscopy. The protocol for embedding of infected tissues was described in Issi et al. (1993). Briefly, small portions of insect tissues were fixed for 2 h at 0 °C in 2.5% (v/v) glutaraldehyde in a 0.1 M phosphate buffer, pH 7.2, washed in the same buffer, and postfixed in 1% (w/v) buffered osmium tetroxide for 1 h. After dehydration in an ethanol series and absolute acetone the fixed tissues were embedded in araldite resin. Sections were stained with uranyl acetate in 70% ethanol and Reynold's lead citrate and examined in a Hitachi H-300 electron microscope. No new sections were taken for our study.

DNA isolation, PCR amplification, and DNA sequencing. For amplification of rDNA sequences, microsporidian DNA was isolated from infected beetles using a QIAmp DNA Mini Kit (Qiagen, Hilden, Germany). The 5′-end of the SSU rRNA gene was amplified with primers V1 (5′-CAC CAG GTT GAT TCT GCC TGA C-3′) and Anncaliiar (5′-ATC GCT TCT ACA TTC ATG CA-3′). The 3′-end of the SSU rRNA gene, the intergenic spacer, and the 5′-end of the LSU rRNA gene were amplified using primers 530f (5′-GTG CCA GC(C/A) GCC GCG G-3′), located in the SSU rRNA gene, and 580r (5′-GGT CCG TGT TTC AAG ACG G-3′), located in the LSU rRNA gene. Primers V1, 530f, and 580r were selected from conserved sequences of the rRNA gene and primer Anncaliiar was designed after sequencing of the 1.5 kb DNA fragment amplified by primers 503f and 580r. Amplifications were done in 50-μl reaction mixtures under the following conditions: 25 pmol of each primer, 200 μM concentration of each deoxynucleoside triphosphate, 10 mM Tris-HCl (pH 9.0), 50 mM KCl, 1.5 mM $MgCl_2$, and 2.5 U of *Taq* DNA polymerase (Roche, Basel, Switzerland). Reactions were run in a Biometra thermocycler (Biometra, Göttingen, Germany) using a step-cycle program. After initial denaturation of DNA at 94 °C for 3 min, 40 cycles were run at 94 °C for 1 min, at 40 °C (V1/Anncaliiar) or 42 °C (530f/580r) for 2 min, and at 72 °C for 3 min, with a 10-min 72 °C extension being carried out after the 40 cycles.

The PCR products were separated on ethidium bromide-stained 1.5% agarose gels and the desired bands were extracted from 1.5% agarose gels by using the QIAquick Gel Extraction Kit (Qiagen). Isolated DNA fragments were directly sequenced on an automated DNA sequencer (ABI PRISM, Applied Biosystems, Foster City, CA) using the primers V1, Anncaliiar, 530f, and 580r. Sequencing of both strands of each PCR fragment was done twice and two PCR products were sequenced for each DNA fragment. The two resulting DNA sequences, representing the 5′-end of the SSU rRNA gene on the one hand, and the 3′-end of the SSU rRNA gene, the intergenic spacer, and the 5′-end of the LSU rRNA gene on the other hand, overlapped for 146 bp and were assembled using GeneTool Lite, version 1.0.

Phylogenetic analysis. Seventeen sequences similar to the SSU rRNA gene sequence of *A. meligethi* were chosen from GenBank using a BLAST search (see Table 1). Fifteen sequences were chosen because of high BLAST scores, while *Nosema bombycis* (GenBank Accession number AB125664) and *Vairimorpha necatrix* (Y00266) were chosen because *A. meligethi* as well as *B. algerae* were originally assigned to the genus *Nosema*. All SSU rRNA gene sequences were automatically aligned on a personal computer using CLUSTAL X, version 1.81 (Thompson et al. 1997) using the default parameter settings and edited visually using BioEdit 7.0.0 (Hall 1999). Phylogenetic analyses using the resultant alignment as the data set were based on the comparison with $\sim$ 1,300 sites from the SSU rRNA gene (variable as well as conserved regions) that were judged to be in alignment.

Phylogenetic analysis of the data sets was done by different algorithms (neighbor-joining, maximum parsimony, and maximum likelihood) using PAUP*, version 4.0 (Swofford 2003). Likelihood settings from the best-fit model were chosen by likelihood ratio tests and AIC criteria in Modeltest 3.6 (Posada and Crandall 1998). The same model (GTR+I+G) was chosen by likelihood ratio tests and AIC criteria and these likelihood settings [Lset Base = (0.2928 0.1578 0.2708) Nst = 6 Rmat = (0.7768 2.2425 1.4809 0.7658 3.7010) Rates = gamma Shape = 0.7456 Pinvar = 0.1189] were used during all likelihood analyses. Several independent calculations were done using different random orders of addition of sequences to increase the probability of finding the shortest or most likely tree. Bootstrap values for all tree-building methods were obtained from 100 resamplings. Consensus trees were calculated by the 50% majority-rule consensus tree method available in PAUP*. *Basidiobolus ranarum* (GenBank Accession number D29946) was used as the outgroup. Handling, manipulation, and plotting of trees was done with TreeView, version 1.6.6. (Page 1996).

RESULTS

Ultrastructure of *Anncaliia meligethi*. Meronts were rounded or elongate. Sometimes they produced characteristic projections protruding deeply into the host cell cytoplasm. The surface coat of meronts possessed a supplementary layer adjacent to the plasmalemma, which consisted of the thin tubules embedded in electron-dense granular material. The overall thickness of the plasma mem-

Table **1.** Hosts and GenBank Accession numbers for the SSU rRNA sequences of 18 microsporidia used in the phylogenetic analyses.

Microsporidium	Host	Accession #
Anncaliia meligethi	*Meligethes aeneus* (Insecta, Coleoptera)	AY894423
Antonospora scoticae	*Andrena scoticae* (Insecta, Hymenoptera)	AF024655
Bacillidium sp.	*Lumbriculus* sp. (Oligochaeta, Lumbriculida)	AF104087
Brachiola algerae	*Homo sapiens* (Mammalia, Primates)	AY230191
Brachiola (Nosema) algerae	*Anopheles stephensi* (Insecta, Diptera)	AF069063
Brachiola (Visvesvaria) algerae	*Anopheles* sp. (Insecta, Diptera)	AF024656
Bryonosema plumatellae	*Plumatella nitens* (Phylactolaemata, Plumatellida)	AF484692
Janacekia debaisieuxi	*Simulium* sp., *Odagmia ornata* (Insecta, Diptera)	AJ252950
Nosema bombycis	*Bombyx mori* (Insecta, Lepidoptera)	AB125664
Paranosema grylli	*Gryllus bimaculatus* (Insecta, Orthoptera)	AY305325
Paranosema locustae	*Locusta migratoria* (Insecta, Orthoptera)	AY305324
Paranosema whitei	*Triboleum* sp. (Insecta, Coleoptera)	AY305323
Pseudonosema cristatellae	*Cristatella mucedo* (Phylactolaemata, Plumatellida)	AF484694
Thelohania solenopsae	*Solenopsis invictae* (Insecta, Hymenoptera)	AF134205
Trichonosema pectinatellae	*Pectinatella magnifica* (Phylactolaemata, Plumatellida)	AF484695
Tubulinosema acridophagus	*Schistocerca americana* (Insecta, Orthoptera)	AF024658
Tubulinosema ratisbonensis	*Drosophila melanogaster* (Insecta, Diptera)	AY695845
Vairimorpha necatrix	*Helicoverpa* sp. (Insecta, Lepidoptera)	Y00266

brane including this layer was 30–50 nm. The parasite cells were also ornamented with characteristic vesicular and tubular structures protruded from the surface into the host cell cytoplasm. The derivates of these secretory structures appeared scattered in the host cell cytoplasm without apparent connection with parasite cell surface (Fig. 1). A supplementary electron-dense layer deposited on the surface of all developmental stages, including the earliest ones, hampered differentiation of meronts and sporonts.

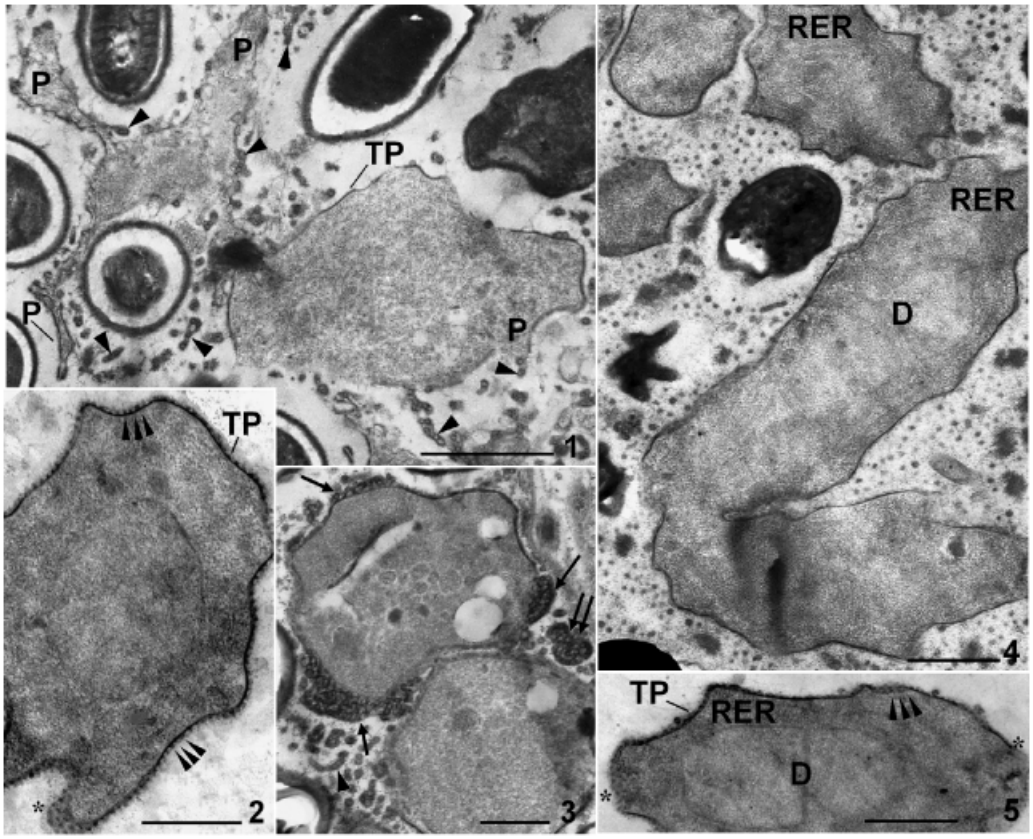

Fig. **1–5.** Ultrastructure of meronts and sporonts of *Anncaliia meligethi*. **1.** Meront with protoplasmic projections (P) protruding into the host cell cytoplasm. Note the thickened plasmalemma (TP) of parasite cell and numerous clusters of vesicles and tubules (arrowheads), which are either attached to the parasite cell or situated freely in the host cell cytoplasm. **2.** Sporont with dense cytoplasm and well-defined TP. Note characteristic electron-dense outer layer with regularly spaced indentations. At some sites (triple arrowheads) TP shows regular array of cross-sectioned electron-transparent tubules embedded in electron-dense matrix. In tangential cuts TP reveals granular texture of electron-dense matrix (asterisks). **3.** Irregular formations (arrows) consisting of electron-dense material with electron-transparent inclusions, which either decorate the cell surface of sporonts (arrow) or appear near the parasite cells (double arrow). **4.** Binary fission of sporont. D-, diplokaryon. **5.** Sporont containing well-defined diplokaryon and the cisterns of rough endoplasmic reticulum (RER). Scale bar: 1.5 μm (Fig. 1), 0.5 μm (Fig. 2–5).

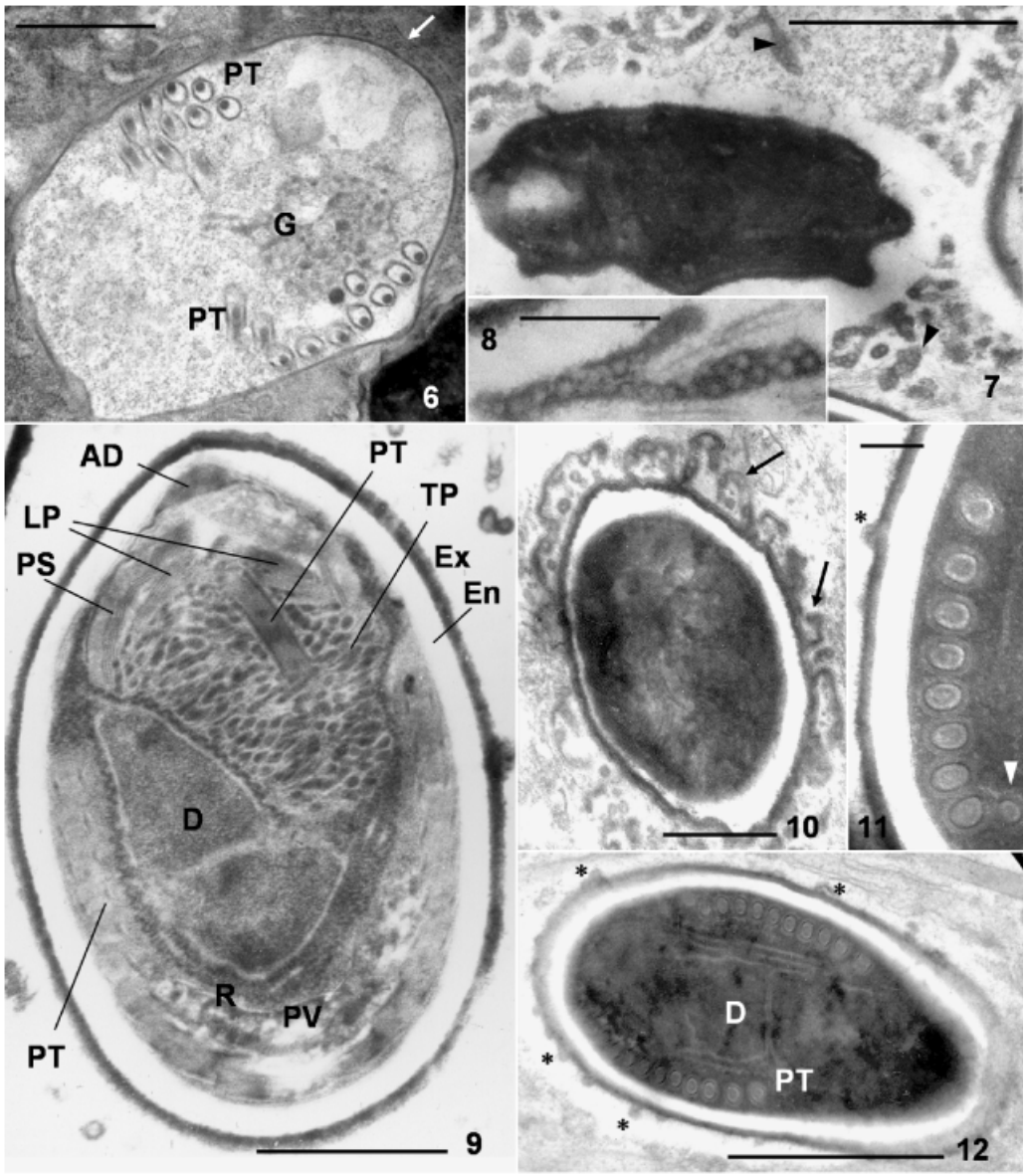

Fig. **6–12.** Ultrastructure of sporoblasts and immature and mature spores of *Anncaliia meligethi*. **6.** Morphogenesis of the polar tube (PT). Sporoblast contains prominent Golgi zone (G) and 9–10 coils of polar filament arranged in three rows. Note the supplementary coating of sporoblast surface consisting of electron-dense matrix with circular inclusions (white arrow). **7.** Clusters and strands of vesicular structures (arrowheads) in the cytoplasm surrounding a late sporoblast. **8.** Higher magnification of a vesicular strand. **9.** Mature spore. AD, anchoring disk; En, endospore; Ex, exospore; LP, lamellar polaroplast; TP, tubular polaroplast; PS, polar sac; PV, posterior vacuole; R, polyribosomes. **10.** Prominent tubular appendages (arrows) on the surface of young spore. **11.** Higher magnification of longitudinal section through a spore revealing anisofilar nature of the polar tube. Note the most distal coil, which has a smaller diameter (white arrowhead) and base of secretory tubular extensions (asterisk). **12.** Secretory tubular extensions (asterisks) of the exospore of not yet fully mature spore. Scale bar: 0.2 μm (Fig. 8, 11), 0.7 μm (Fig. 6, 9–10), 1.5 μm (Fig. 7, 12).

Transition to sporogony was marked with (1) an increase in the electron density of the parasite cytoplasm; (2) progressive development of the rough endoplasmic reticulum; (3) augmentation of the granulotubular layer; and (4) progressive accumulation of the tubular and vesicular structures in the host cell cytoplasm (Fig. 2–5).

Compared with the earlier developmental stages, sporonts and early sporoblasts had denser cytoplasm and well-defined thickened plasmalemma, coated with the electron-dense outer layer with regularly spaced indentations. In certain sites, the indented profile of the cell coat appeared to be because of the presence of regular arrays of electron-transparent tubules embedded in the electron-dense granular matrix (Fig. 2, 5). Irregular formations consisting of electron-dense material with electron-transparent inclusions were attached to the sporont surface at some sites or appeared near the parasite cells (Fig. 3). Both meronts and sporonts were diplokaryotic and divided by binary fission; sporogony was disporoblastic (Fig. 4, 5).

Sporoblasts contained a prominent Golgi zone and 9–10 coils of the polar tube arranged in three rows. The sporoblast surface possessed an unusual supplementary coating consisting of an electron-dense matrix with circular inclusions (Fig. 6). Strands and irregular clusters of vesicles were scattered in the cytoplasm surrounding the sporoblasts (Fig. 7, 8).

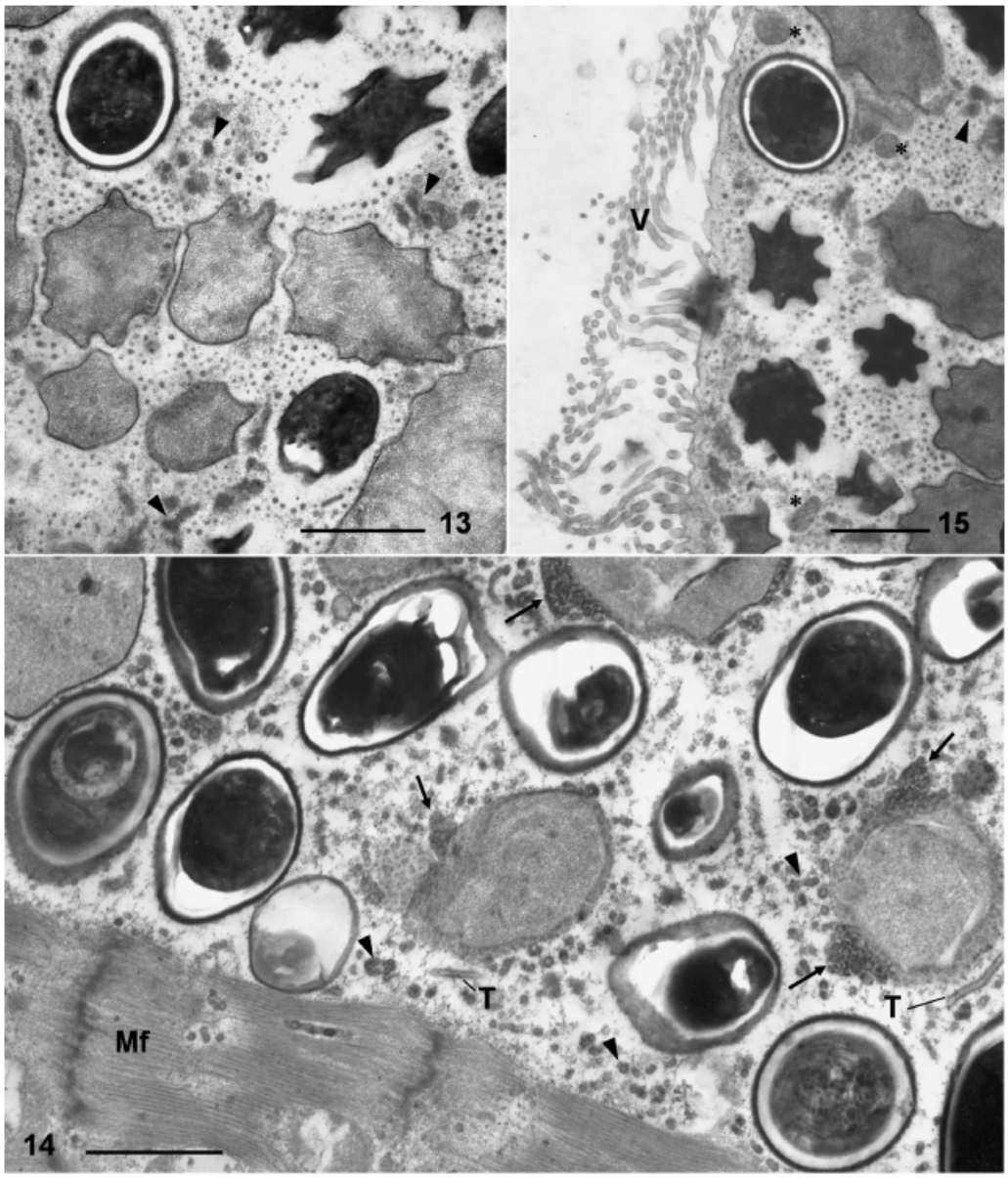

Fig. **13–15.** Intracellular development of *Anncaliia meligethi* in the type host (13, 14) and in a non-specific host (15). **13.** Development of *A. meligethi* in the cells of the fat body of the type host *Meligethes aeneus*. Note numerous solitary vesicles and variously shaped vesicular structures (arrowheads) abundant in the surrounding host cell cytoplasm. **14.** Development of *A. meligethi* in the sarcoplasm of muscles of *M. aeneus*. Mf, striated muscle filaments. Note abundant vesicles, the single tubules (T), vesicular structures (arrowheads), and irregular formations similar to the structures indicated in Fig. 2 (arrow*s*). **15.** Development of *A. meligethi* in the intestinal epithelium of the caterpillar of a non-specific host, *Pieris brassicae*. V, villi of intestine epithelium. Vesicles and vesicular structures (arrowheads) can also be seen in this host's cytoplasm. The heavy destruction of the host cell cytoplasm is evident, mitochondria represent the only host organelles, which are still recognizable (asterisks). Scale bar: 1.5 μm.

Spores were oval and diplokaryotic (Fig. 9). The endospore of the mature spores was rather thick: 120 nm on average with a minimal thickness of 30 nm at the anterior spore pole above anchoring disk. The exospore was up to 60 nm thick and composed of two layers. The inner one was thicker and had higher electron density. The outer one was thinner and less electron-dense, and was ornamented by tubules, radiating perpendicularly to the longitudinal axis of the spore into the host cell cytoplasm (Fig. 10). These tubules were especially prominent at the anterior and posterior poles and at the equatorial part of the spore. The outer tubular layer was more conspicuous in young spores (Fig. 10), but the points where the tubules radiated from the exospore remained visible in mature spores (Fig. 11, 12). The anchoring disk was mushroom-shaped, up to 370 nm in diam. The trilaminar polar sac, 120 nm thick, surrounded the anterior part of the polaroplast. The polaroplast was bipartite and consisted of an anterior lamellar part and posterior tubular one. The anterior nucleus of the diplokaryon was flattened toward the polaroplast and nearly conical shaped, while the posterior nucleus was hemispherical (Fig. 9). The polar tube was slightly anisofilar and formed 13–15 coils with 3–4 distal coils of a smaller diam. arranged in a single row (Fig. 11, 12).

Parasite development was observed in the fat body and in the sarcoplasm of muscles of *M. aeneus,* the type host of this micro-

sporidium (Fig. 13, 14). In specimens of the experimentally infected non-specific host, the caterpillars *P. brassicae,* parasite proliferation and spore production occurred in the intestine epithelium (Fig. 15). In all tissues parasites developed in direct contact with the host cell cytoplasm. Electron-transparent zones of the host cell cytoplasm appeared around all developmental stages of *A. meligethi*, while the rest of the cytoplasm was filled with numerous solitary vesicles and tubules, as well as with variously shaped clusters of tubular and vesicular structures (Fig. 1, 2, 7, 8, 13–15). The mitochondria and muscle fibers were the only host organelles that remained recognizable in the infected host cells (Fig. 15). Heavy destruction of the host cell was found in all studied cases, irrespective of the infected host species and the site of infection (Fig. 13–15).

Ribosomal RNA sequence. A ~1.5-kb DNA band was amplified from genomic DNA preparations of air-dried infected beetles by PCR using primers 530f and 580r. Sequencing of this DNA fragment utilizing primers 530f and 580r provided a 1,444-bp DNA sequence. A ~ 580-bp DNA band was amplified from the genomic DNA preparations using primers V1 and Anncaliiar and sequencing provided a 578-bp DNA sequence. These two DNA sequences overlapped for 146 bps and were assembled. The resulting consensus DNA sequence of the complete SSU rRNA gene, the intergenic spacer region, and the 5′-end of the LSU rRNA gene of *A. meligethi* was submitted to the GenBank database under Accession no. AY894423. This rRNA sequence was 1,876 bp in length with a GC content of 47.1%. A BLAST search of the GenBank database with the sequence obtained from *A. meligethi* detected close matches to other microsporidian rRNA sequences. The rRNA sequence of *A. meligethi* showed 96.7% sequence identity with a 1,878-bp fragment containing the whole SSU rRNA, the intergenic spacer, and the 5′-end of the LSU rRNA of *B. algerae* (Accession nos. AY230191 and AF069063) and 98.6% identity with a 1,366-bp SSU rRNA sequence submitted to the GenBank database as *Visvesvaria algerae* (AF024656). The LSU rRNA 580r region of *A. meligethi* showed 91.5% sequence identity with a 344-bp DNA fragment of *B. algerae* (L28961).

Phylogenetic analysis based on small subunit rRNA sequence. All methods (likelihood, parsimony, distance) applied to the SSU rRNA gene sequence alignment revealed the same general tree topology: in all trees *A. meligethi* clustered with the three sequences of *B. algerae* (AY230191, AF069063, and AF024656) (Fig. 16). Bootstrap values for this node were 100% for distance, parsimony, and likelihood methods and also for the node establishing the genera *Thelohania* and *Tubulinosema* as sister clades to that containing *A. meligethi* (Fig. 16). In no case did *N. bombycis* cluster with *A. meligethi* or *Brachiola* spp. Other branches of the trees were above 60% (Fig. 16).

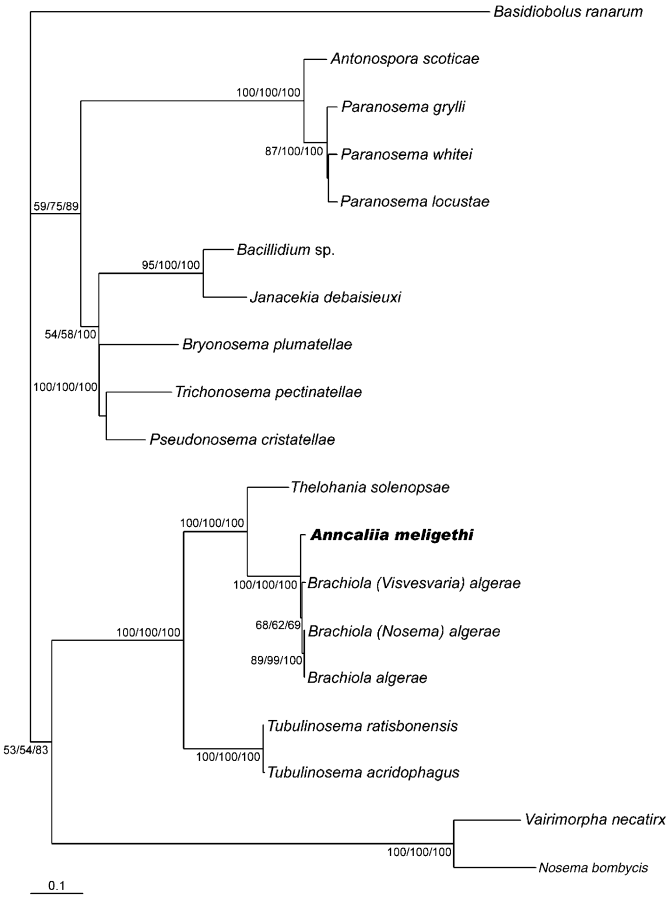

Fig. **16.** Maximum likelihood analysis of small subunit rRNA of *Anncaliia meligethi* showing its relationsip to *Brachiola algerae*. *Tubulinosema* forms a sister taxon to this group. The true *Nosema* spp. including *Nosema bombycis* do not fall into the clade with *A. meligethi* and *B. algerae*. Bootstrap values on the tree (likelihood, parsimony, and distance analysis, respectively, at each node) are from other analyses that provided identical topology.

DISCUSSION

Even a brief look shows that many morphological features characteristic of *A. meligethi* have been reported from various *Brachiola* species. For example, a supplementary granulotubular layer deposited on the surface of proliferative stages of *A. meligethi* is seemingly homologous with the ''thick, electron-dense coating'' encrusting the plasmalemma of *B. vesicularum* (see Fig. 14–16 in Cali et al. 1998) and with ''tubular fleece'' on the cell surface of *B. algerae* (see Fig. 1B, E, 2B in Koudela et al. 2001; Fig. 16, 20 in Vávra and Undeen, 1970). Clusters of tubular and vesicular structures decorating the cell surface of *A. meligethi* and appearing scattered in the host cell cytoplasm resemble ''vesiculotubular appendages'' of *B. vesicularum* (see Fig. 18–21 in Cali et al. 1998), ''tubulo-vesicular tuft'' and ''tubulo-vesicular channels'' of *B. algerae* (see Fig. 1F, G, 2F, 3C in Koudela et al. 2001). Irregular formations consisting of electron-dense material with electron-transparent inclusions found in electron micrographs of *A. meligethi* look very similar to the structures described as ''irregular accumulations of the fibrous and vesiculotubular material extensively protruding off of small areas'' of the cell surface of *B. vesicularum* (see Fig. 23–24 in Cali et al. 1998; Fig. 8–10 in Cali et al. 2004) or as ''irregular blebs of electron-dense material with circular electron-lucent inclusions'' in *B. algerae* (see Fig. 2D in Koudela et al. 2001). Distinguishing characters of *B. vesicularum* are the ''elongated protoplasmic extensions'' (see Fig. 26–29 in Cali et al. 1998). We observed similar cytoplasmic protrusions, although probably less developed, in electron micrographs of meronts of *A. meligethi*.

Comparison with longitudinal sections through mature spores of *B. vesicularum* (see Fig. 9–13 in Cali et al. 1998) and of *B. algerae* (see Fig. 2 in Chioralia et al. 1998; Fig. 1, 3, 5 in Cali, Weiss, and Takvorian 2002) with those of *A. meligethi* demonstrates the close similarity of spore ultrastructure. In all these species the polaroplast is bipartite and the polar tube is slightly anisofilar. The coils are arranged in a single row in both *A. meligethi* and in *B. algerae*. Cali et al. (1998) reported that the polar tube in the spores of *B. vesicularum* formed 7–10 coils typically clustered in a double row. However, arrangements in a triple or

Table **2.** Morphological features of the species of the emended genus *Anncaliia.*

Species	Spore size (μm)	Polar tube: number of coils; rows; distal narrower coils	Nuclear polymorphism in the spore	Protoplasmic extensions	References
A. meligethi	4–5 × 2–3	13–15; 1; 3–4	+	+	Issi and Radishcheva (1979), Issi, Krylova, & Nicolaeva (1993)
A. algerae	3.7–5.4 × 2.3–3.9[a]	8–11; 1; 0–3[b]	+[c]	–	Avery and Anthony (1983), Cali, Weiss, and Takvorian (2002, 2004)[b]; Canning and Hulls (1970), Canning and Sinden (1973), Chioralia et al. (1998)[c], Koudela et al. (2001)[b], Lowman, Takvorian, and Cali (2000), Vávra and Undeen (1970)[a]
A. connori	4.0–4.5 × 2.0–2.5	10–12; 1; ?	?	?	Margileth et al. (1973), Shadduck, Kelsoe, and Helmke (1979), Sprague (1974), Strano et al. (1976)
A. gambiae	2.5–3.0 × 1.5–2.0	9; 1; 3–4	?	?	Fox and Weiser (1959), Weiser and Žižka (2004)
A. varivestis	4.6–4.8 × 2.6	17–19; 1; ?	?	?	Brooks et al. (1980), Brooks, Hazard, and Becnel (1985)
A. vesicularum	2.5 × 2.0	7–10; 1–3 (2); 2–3	?	+	Cali et al. (1998)

''?''—Not known (not specified in the published papers or not clear from the published images).
[a,b,c]Indicate the reference to the data; it is done in case of contradictions among different authors.

single row of coils were also observed. The arrangement of coils in the polar tube is apparently a rather variable character. Variable arrangements of polar tube coils were observed in *B. algerae* cultivated at temperatures between 29 °C and 38 °C (Lowman et al. 2000; Trammer et al. 1999). Trammer et al. (1999) suggested that the number and the arrangement of polar tube coils might be host cell- and temperature-dependant.

Host cell reactions to development of *Anncaliia* and *Brachiola* species are very similar. Heavy destruction of host cytoplasm was noted in all papers devoted to ultrastructural and developmental features of both *Anncaliia* spp. and *Brachiola* spp. (e.g. Brooks et al. 1985; Cali et al. 1998; Issi et al. 1993; Vávra and Undeen 1970). The cytoplasm is lysed to an extent proportional to parasite proliferation and spore maturation. The content of the host cell becomes electron-transparent. Only mitochondria, muscle fibers, and sometimes endoplasmic reticulum remained recognizable in the infected host cells. Cali et al. (1998) noted that the disappearance of host cell organelles is extremely localized to the specific area of vesiculotubular parasite appendages.

Comparative analysis of ultrastructural organization of *A. meligethi* with that of *B. vesicularum* and *B. algerae* clearly demonstrates that *Anncaliia* and *Brachiola* species share many distinctive morphological features. Therefore, details of the ultrastructural data support the close relatedness of these genera (Table 2) as do features of their biology (Table 3).

We amplified a 1,876-bp fragment of rDNA unit from genomic DNA isolated from archival air-dried specimens of *M. aeneus* infected with *A. meligethi*. To our knowledge this is the first successful amplification of ancient microsporidian DNA from air-dried host cadavers stored for a long time. There are no molecular data available for *B. vesicularum*, the type species of the genus *Brachiola*, nor for other members of this genus (*B. connori*, *B. gambiae*) except for *B. algerae*. This genus was established after ultrastructural examination of the parasites in a biopsy specimen; PCR amplification of DNA from the tissue failed (Cali et al. 1998). Our phylogenetic analysis showed strong similarities between the sequences of *A. meligethi* and *B. algerae*, and these two species always clustered together with a 100% bootstrap support by all methods.

The combined ultrastructural and molecular data clearly indicate that *A. meligethi* and *B. algerae* are very closely related. We consider them as congeneric species. This warrants emendation of the genus *Anncaliia* with inclusion of all species of the genus *Brachiola*, and we establish the new combinations below (see Taxonomic Summary). The International Code of Zoological Nomenclature (1999) supports the generic name *Anncaliia* Issi, Krylova, & Nicolaeva 1993 over *Brachiola* Cali, Takvorian, Lewin, Rendel, Sian, Wittner, Tanowitz, Keohane, & Weiss 1998, based on the Principle of Priority (article 23.3).

The clade containing *Anncaliia* spp. forms a sister clade to *Tubulinosema* spp. The most characteristic ultrastructural features shared by these genera, are tubular ornamentation of the cell surface in the proliferative stages and a slightly anisofilar polar tube. These characters are among the principal ones for the recently established family Tubulinosematidae Franzen, Fischer, Schroeder, Schölmerich, & Schneuwly 2005. Molecular and ultrastructural similarities support the placement of the genus *Anncaliia* in this family. We must exclude *Thelohania* from this family on morphological grounds (the sporonts of *Thelohania* undergo octosporoblastic sporogony and the uninucleated spores are contained within a sporophorous vesicle), although this genus at present falls into the same molecular clade. We predict that when additional DNA data from other genes and from a greater number of microsporidian species are included, phylogenetic analyses will show that *Thelohania* is not closely related to the microsporidia that produce tubuli on the surface of their meronts.

Beside the important outcomes for microsporidian systematics, our data provide one more example of an insect parasite that is phylogenetically related to a human-infecting species. It is an interesting finding in the light of possible transmission of microsporidia from insects and other invertebrate hosts to vertebrates, especially to mammals, and it shows the weakness of such physiological characters as thermotolerance for microsporidian systematics. Many microsporidia are characterized by a wide host range and are highly adaptive: they can invade various hosts with very different physiological temperature optima. High sequence homology between coleopteran-, dipteran-, and human-infecting species suggests a high plasticity of *Anncaliia* spp.

Table **3.** Comparative biology of the emended genus *Anncaliia*.

Species	Sites of infection	Host range	Thermotolerance	Prevalence	References
A. meligethi	Muscles and fat body in the type host, intestine epithelium and fat body in a non-specific host	Insects (Coleoptera, in experiment Lepidoptera[a])	Not studied	From 1975 to 1993 continuous monitoring in populations of *Meligethes aeneus* in Northwest region of Russia, Ukraine, and Estonia[b]; regular isolation in Denmark, Finland, and Sweden[c]	Hokkanen and Lipa (1991, 1995)[c], Issi and Radishcheva (1979)[b], Issi et al. (1993)[a,b], Lipa and Ekbom (2003)[c], Lipa and Hokkanen (1991, 1992)[c]
A. algerae	Generalized infection (insects); footpads, tail, ears, liver (mice), eyes, quadriceps muscle (human)	Insects (Diptera) and mammals; in experiment[d] many invertebrate and vertebrate hosts; maintenance in insect[e] and vertebrate[f] cell cultures	Thermo-tolerant	Frequent appearance in laboratory and natural populations of mosquitoes[g]. Type isolate CDC: V427 found in USA in 1966 in a laboratory colony of *Anopheles stephensi*[h]. There are human isolates: CDC: V404 from infected corneal scrapings of an HIV-negative 67-year-old man[i], CDC: V422 from a skin lesion in a child with acute lymphocytic anemia[j] and ATCC-PRA109 from a muscle biopsy of a patient treated with immunosuppressive drugs[k]	Alger and Undeen (1970)[h], Cali et al. (2004)[d,f], Coyle et al. (2004)[k], Canning and Hulls (1970)[g], Canning and Sinden (1973)[g], Koudela et al. (2001)[d], Kucerova et al. (2004)[j], Lowman et al. (2000), Moura et al. (1999)[f], Smith, Barker, and Lai (1982)[f], Streett, Ralph, and Hink (1980)[e]; Trammer et al. (1997, 1999)[f], Undeen (1975)[f], Undeen and Alger (1976)[d], Undeen and Maddox (1973)[d], Vávra and Undeen (1970), Visvesvara et al. (1999)[i]
A. connori	Epithelial, connective and muscle tissue	Human	Thermo-tolerant	Single case of systemic infection occured in a 4-month-old thymus-deficient infant	Margileth et al. (1973), Shadduck, Kelsoe, and Helmke (1979), Sprague (1974), Strano, Cali, and Neafie (1976)
A. gambiae	Generalized infection	Insects (Diptera)	Not studied	Epizooty in a mosquito colony of *Anopheles gambiae* in Liberia in 1956; occurence in natural host populations	Fox and Weiser (1959), Weiser and Žižka (2004)
A. varivestis	Generalized infection (except for midgut epithelium), significant parasite development occurs only in the Malpigian tubules	Insects (Coleoptera)	Not studied	Occurence in laboratory and field-collected colonies of *Epilachna varivestis* in North and South Carolina, USA	Brooks et al. 1980, 1985
A. vesicularum	Skeletal muscles	Human	Thermo-tolerant	Single case of infection found in biopsied muscle tissue of HIV patient	Cali et al. (1998)

[a-k]indicate the reference to the data.

Taxonomic Summary

Anncaliia Issi, Krylova & Nicolaeva 1993 emend.

Monoxenic, monomorphic, diplokaryotic, disporoblastic. Meiosis unknown. Multiplication by binary fission. Transmission per os (transmission unknown for human-infecting species). Development takes place in direct contact with host cell cytoplasm. Proliferative stages, including sporoplasms, with electron-dense granulotubular layer on the outer surface of plasmalemma producing the ''thickened plasmalemma'' appearance. In some species (*A. meligethi*, *A. vesicularum*) proliferative stages produce protoplasmic extensions, deeply penetrating into the host cell cytoplasm. In proliferative and sporogonic stages, the parasite elaborates a complex of extracellular secretory structures, called vesiculotubular appendages. These structures occur on the cell surface or in the surrounding host cell cytoplasm without apparent connection with parasite cell surface. Vesiculotubular appendages disappear only in mature spores, but the bases of these tubules remain visible on the surface of exospore. Spores are diplokaryotic, oval to pyriform, and less than 5 μm in size. The polar tube is slightly anisofilar with one to four distal coils having a smaller diameter. The polaroplast is bipartite with anterior lamellar and posterior tubular parts. Shape polymorphism of the nuclei in the spore diplokaryon is reported in *A. meligethi* and *A. algerae*. The cytoplasm of infected cells is heavily destroyed and electron-transparent.

Host range. Parasites of Coleoptera: Nitidulidae, Coccinellidae; Diptera: Culicidae; Primates: Hominidae. Experimental infections of lepidopterans with *A. meligethi* demonstrated a potentially wide host range of this species. *Anncaliia algerae* has been identified both in insects and in human.

Type species. *Anncaliia meligethi* (Issi & Radishcheva 1979) Issi et al. 1993.

Type host. *Meligethes aeneus* (Coleoptera, Nitidulidae).

Etymology. The genus *Anncaliia* was named in the honor of Ann Cali who gave the first detailed ultrastructural description of *Nosema bombycis*, type species of the genus *Nosema*, and suggested the new diagnostic criteria for this genus (Cali 1971).

Synopsis of the emended genus *Anncaliia*.

Anncaliia meligethi (syn. *Nosema meligethi* Issi & Radishcheva 1979) Issi, Krylova, & Nicolaeva 1993.
Anncaliia algerae (syn. *Nosema algerae* Vávra & Undeen 1970; syn. *Brachiola algerae* Lowman, Takvorian, & Cali 2000) nov. comb.
Anncaliia connori (syn. *Nosema connori* Sprague 1974; *Brachiola connori* Cali, Takvorian, Lewin, Rendel, Sian, Wittner, Tanowitz, Keohane, & Weiss 1998) nov. comb.
Anncaliia gambiae (syn. *Nosema* cf. *stegomyiae* sensu Fox & Weiser 1959; syn. *Brachiola gambiae* Weiser & Žižka 2004) nov. comb.

Anncaliia varivestis (syn. *Nosema varivestis* Brooks et al. 1985) Issi, Krylova, & Nicolaeva 1993.
Anncaliia vesicularum (syn. *Brachiola vesicularum* Cali, Takvorian, Lewin, Rendel, Sian, Wittner, Tanowitz, Keohane, & Weiss 1998) nov. comb.

ACKNOWLEDGMENTS

This study was supported by a grant from the Bundesministerium für Bildung und Forschung, (BMBF)-Programm zur Förderung von Klinischen Forschergruppen in der Klinischen Infektiologie, Förderkennzeichen 01 KI 9952 and by RFBR (Russian Foundation for Basic Research) grant nos. 04-04-49314, 04-04-49209, and 05-04-49222.

LITERATURE CITED

Alger, N. E. & Undeen, A. H. 1970. The control of a microsporidian, *Nosema* sp., in an anopheline colony by an egg-rinsing technique. *J. Invertebr. Pathol.*, **15**:321–327.

Avery, S. W. & Anthony, D. W. 1983. Ultrastructural study of early development of *Nosema algerae* in *Anopheles albimanus*. *J. Invertebr. Pathol.*, **42**:87–95.

Baker, M. D., Vossbrinck, C. R., Maddox, J. V. & Undeen, A. H. 1994. Phylogenetic relationships among *Vairimorpha* and *Nosema* species (Microspora) based on ribosomal RNA sequence data. *J. Invertebr. Pathol.*, **64**:100–106.

Brooks, W. M., Hazard, E. I. & Becnel, J. 1985. Two new species of *Nosema* (Microsporida: Nosematidae) from the Mexican bean beetle *Epilachna varivestis* (Coleoptera: Coccinellidae). *J. Protozool.*, **32**:525–535.

Brooks, W. M., Montross, D. B., Sprenkel, R. K. & Carner, G. 1980. Microsporidioses of coleopterous pests of soybeans. *J. Invertebr. Pathol.*, **35**:93–95.

Cali, A. 1971. Morphogenesis in the genus *Nosema*. Proceedings of the IV International Colloqium in Insect Pathology, College Park, MD, 1970. p. 431–438.

Cali, A., Weiss, L. M. & Takvorian, P. M. 2002. *Brachiola algerae* spore membrane systems, their activity during extrusion, and a new structural entity, the multilayered interlaced network, associated with the polar tube and the sporoplasm. *J. Eukaryot. Microbiol.*, **49**:164–174.

Cali, A., Weiss, L. M. & Takvorian, P. M. 2004. An analysis of the microsporidian genus *Brachiola*, with comparisons of human and insect isolates of *Brachiola algerae*. *J. Eukaryot. Microbiol.*, **51**:678–685.

Cali, A., Takvorian, P. M., Lewin, S., Rendel, M., Sian, C. S., Wittner, M., Tanowitz, H. B., Keohane, E. & Weiss, L. M. 1998. *Brachiola vesicularum*, n. g., n. sp., a new microsporidium associated with AIDS and myositis. *J. Eukaryot. Microbiol.*, **45**:240–251.

Canning, E. U. & Hulls, R. H. 1970. A microsporidan infection of *Anopheles gambiae* Giles, from Tanzania, interpretation of its mode of transmission and notes on *Nosema* infections in mosquitoes. *J. Protozool.*, **17**:531–539.

Canning, E. U. & Sinden, R. E. 1973. Ultrastructural observations on the development of *Nosema algerae* Vávra and Undeen (Microsporida, Nosematidae) in the mosquito *Anopheles stephensi* Liston. *Protistologica*, **9**:405–415.

Chioralia, G., Trammer, T., Maier, W. A. & Seitz, H. M. 1998. Morphologic changes in *Nosema algerae* (Microspora) during extrusion. *Parasitol. Res.*, **84**:123–131.

Coyle, C. M., Weiss, L. M., Rhodes, L. V. III, Cali, A., Takvorian, P. M., Brown, D. F., Visvesvara, G. S., Xiao, L., Naktin, J., Young, E., Gareca, M., Colasante, G. & Wittner, M. 2004. Fatal myositis due to the microsporidian *Brachiola algerae*, a mosquito pathogen. *N. Engl. J. Med.*, **351**:42–47.

Fox, R. M. & Weiser, J. 1959. A microsporidian parasite of *Anopheles gambiae* in Liberia. *J. Parasitol.*, **45**:21–30.

Franzen, C., Fischer, S., Schroeder, J., Schölmerich, J. & Schneuwly, S. 2005. Morphological and molecular investigations of *Tubulinosema ratisbonensis* gen. nov., sp., nov. (Microsporidia: Tubulinosematidae fam. nov.), a parasite infecting a laboratory colony of *Drosophila melanogaster* (Diptera: Drosophilidae). *J. Eukaryot. Microbiol.*, **52**: 141–152.

Hall, T. A. 1999. BioEdit: a user-friendly biological sequence alignment editor and analysis program for Windows 95/98/NT. *Nucelic Acids Symp. Ser*, **41**:95–98.

Hokkanen, H. M. T. & Lipa, J. J. 1991. Ecology of *Nosema meligethi* (Microsporida) as a parasite of *Meligethes aeneus* (Coleoptera, Nitidulidae). *IOBC/WPRS Bull. OILB/SROP*, **14**:90–95.

Hokkanen, H. M. T. & Lipa, J. J. 1995. Occurrence and dynamics of *Nosema meligethi* (Microsporida) in populations of *Meligethes aeneus* (Coleoptera, Nitidulidae) in Finland. *Entomol. Fenn.*, **6**:11–18.

International Comission on Zoological Nomenclature. 1999. International Code of Zoological Nomenclature, 4th ed. The International Trust for Zoological Nomenclature c/o The Natural History Museum. London, UK.

Issi, I. V. & Radishcheva, D. F. 1979. Microsporidioses of the beetle pests of cruciferous cultures in Leningrad region. *Bull. All-Union Ins. Plant Protection*, **46**:19–23. (in Russian)

Issi, I. V., Krylova, S. V. & Nicolaeva, V. M. 1993. The ultrastructure of the microsporidium *Nosema meligethi* and establishment of the new genus *Anncaliia*. *Parazitologiia*, **27**:127–133. (in Russian with English summary)

Koudela, B., Visvesvara, G. S., Moura, H. & Vávra, J. 2001. The human isolate of *Brachiola algerae* (Phylum Microspora): development in SCID mice and description of its fine structure features. *Parasitology*, **123**:153–162.

Kucerova, Z., Moura, H., Visvesvara, G. S. & Leitch, G. J. 2004. Differences between *Brachiola* (*Nosema*) *algerae* isolates of human and insect origin when tested using an in vitro spore germination assay and a cultured cell infection assay. *J. Eukaryot. Microbiol.*, **51**:339–343.

Lipa, J. & Ebkom, B. 2003. Microsporidian, haplosporidian, and eugregarine parasites present in populations of *Meligethes aeneus* F. in Sweden. *Acta Agric. Scand.*, Sect. B, Soil Plant Sci., **53**:87–89.

Lipa, J. J. & Hokkanen, H. M. T. 1991. A haplosporidian *Haplosporidium meligethi* sp. n., and a microsporidian *Nosema meligethi* I. et R., two protozoan parasites from *Meligethes aeneus* F. (Coleoptera: Nitidulidae). *Acta Protozool.*, **30**:217–222.

Lipa, J. J. & Hokkanen, H. M. T. 1992. *Nosema meligethi* I. et R. (Microsporida) in populations of *Meligethes* spp. in Europe. *Biocontrol. Sci. Technol.*, **2**:19–125.

Lowman, P. M., Takvorian, P. M. & Cali, A. 2000. The effects of elevated temperatures and various time–temperature combinations on the development of *Brachiola* (*Nosema*) *algerae* n. comb. in mammalian cell culture. *J. Eukaryot. Microbiol.*, **47**:221–234.

Margileth, A. M., Strano, A. J., Chandra, R., Neafie, R., Blum, M. & McCully, R. M. 1973. Dissiminated nosematosis in an immunologically compromised infant. *Arch. Pathol.*, **95**:145–150.

Moura, H., da Silva, A., Moura, I. N. S., Schwartz, D. A., Leitch, G., Wallace, S., Pieniazek, N. J., Wirtz, R. A. & Visvesvara, G. S. 1999. Characterization of *Nosema algerae* isolates after continuous cultivation in mammalian cells at 37 °C. *J. Eukaryot. Microbiol.*, **46**:14S–16S.

Müller, A., Trammer, T., Chioralia, G., Seitz, H. M., Diehl, V. & Franzen, C. 2000. Ribosomal RNA of *Nosema algerae* and phylogenetic relationship to other microsporidia. *Parasitol. Res.*, **86**:18–23.

Page, R. D. M. 1996. TREEVIEW: an application to display phylogenetic trees on personal computers. *Comput. Appl. Biosci.*, **12**:357–358.

Posada, D. & Crandall, K. A. 1998. MODELTEST: testing the model of DNA substitution. *Bioinformatics*, **14**:817–818.

Shadduck, J. A., Kelsoe, G. & Helmke, R. J. 1979. A microsporidian contaminant of a non-human primate cell culture: ultrastructural comparison with *Nosema connori*. *J. Parasitol.*, **65**:185–188.

Smith, J. E., Barker, R. J. & Lai, P. F. 1982. Culture of microsporidia from invertebrates in vertebrate cells. *Parasitology*, **85**:427–435.

Sprague, V. 1974. *Nosema connori* n. sp., a microsporidian parasite of man. *Trans. Am. Microsc. Soc.*, **93**:400–403.

Strano, A. J., Cali, A. & Neafie, R. C. 1976. Microsporidiosis. *In*: Binford, C. H. & Connor, D. H. (ed.), Pathology of Tropical and Extraordinary Diseases, An Atlas, Vol. I. Armed Forces Institute of Pathology Press, Washington, DC. **14**:336–339.

Streett, D. A., Ralph, D. & Hink, W. F. 1980. Replication of *Nosema algerae* in three insect cell lines. *J. Protozool.*, **27**:113–117.

Swofford, D. L. 2003. PAUP*. Phylogenetic Analysis using Pasimony (* and other Methods), v. 4.0b10. Sinauer Associates, Sunderland, MA, USA.

Thompson, J. D., Gibson, T. J., Plewniak, F., Jeanmougin, F. & Higgins, D. G. 1997. The CLUSTAL_X windows interface: flexible strategies for multiple sequence alignment aided by quality analysis tools. *Nucleic Acids Res.*, **25**:4876–4882.

Trammer, T., Chioralia, G., Maier, W. A. & Seitz, H. M. 1999. In vitro replication of *Nosema algerae* (Microsporidia), a parasite of anopheline mosquitoes, in human cells above 36 °C. *J. Eukaryot. Microbiol.*, **46**:464–468.

Trammer, T., Dombrowski, F., Doehring, M., Maier, W. A. & Seitz, H. M. 1997. Opportunistic properties of *Nosema algerae* (Microspora), a mosquito parasite, in immunocompromised mice. *J. Eukaryot. Microbiol.*, **44**:258–262.

Undeen, A. H. 1975. Growth of *Nosema algerae* in pig kidney cell cultures. *J. Protozool.*, **22**:107–110.

Undeen, A. H. & Alger, N. E. 1976. *Nosema algerae*: infection of the white mouse by a mosquito parasite. *Exp. Parasitol.*, **40**:86–88.

Undeen, A. H. & Maddox, J. V. 1973. The infection of non-mosquito hosts by injection with spores of the microsporidian *Nosema algerae*. *J. Invertebr. Pathol.*, **22**:258–265.

Vávra, J. & Undeen, A. H. 1970. *Nosema algerae* n. sp. (Cnidospora, Microsporida) a pathogen in a laboratory colony of *Anopheles stephensi* Liston (Diptera, Culicidae). *J. Protozool.*, **17**:240–249.

Visvesvara, G. S., Belloso, M., Moura, H., Da Silva, A., Moura, I., Leitch, G., Schwartz, D. A., Chevezbarrious, P., Wallace, S., Pieniazek, N. J. & Goosey, J. 1999. Isolation of *Nosema algerae* from the cornea of an immunocompetent patient. *J. Eukaryot. Microbiol.*, **46**:10S.

Weiser, J. & Žižka, Z. 2004. *Brachiola gambiae* sp. n., the microsporidian parasite of *Anopheles gambiae* and *A. melas* in Liberia. *Acta Protozool.*, **43**:73–80.

Received: 03/10/05, 06/02/05; accepted: 08/30/05